Taylor & Francis
Taylor & Francis Group

Corrosion Engineering, Science and Technology

The International Journal of Corrosion Processes and Corrosion Control

ISSN: 1478-422X (Print) 1743-2782 (Online) Journal homepage: http://www.tandfonline.com/loi/ycst20

Effects of different inorganic anions on equipment material corrosion behaviour in subcritical water oxidation

Wenjing Sun, Huangzhao Wei, Xianru Li, Zi-ang Xiong & Chenglin Sun

To cite this article: Wenjing Sun, Huangzhao Wei, Xianru Li, Zi-ang Xiong & Chenglin Sun (2018) Effects of different inorganic anions on equipment material corrosion behaviour in subcritical water oxidation, Corrosion Engineering, Science and Technology, 53:6, 403-412, DOI: 10.1080/1478422X.2018.1495143

To link to this article: https://doi.org/10.1080/1478422X.2018.1495143

Published online: 09 Jul 2018.

Submit your article to this journal

Article views: 20

View Crossmark data

Full Terms & Conditions of access and use can be found at
http://www.tandfonline.com/action/journalInformation?journalCode=ycst20

CORROSION ENGINEERING, SCIENCE AND TECHNOLOGY
2018, VOL. 53, NO. 6, 403–412
https://doi.org/10.1080/1478422X.2018.1495143

The Institute of Materials, Minerals and Mining

Taylor & Francis
Taylor & Francis Group

Check for updates

Effects of different inorganic anions on equipment material corrosion behaviour in subcritical water oxidation

Wenjing Sun[a,b], Huangzhao Wei[a], Xianru Li[c], Zi-ang Xiong[d] and Chenglin Sun[a]

[a]Dalian Institute of Chemical Physics, Chinese Academy of Sciences, Dalian, People's Republic of China; [b]University of Chinese Academy of Sciences, Beijing, People's Republic of China; [c]Zhangjiagang Industrial Technology Research Institute Co., Ltd, Dalian Institute of Chemical Physics, Chinese Academy of Sciences, Zhangjiagang, People's Republic of China; [d]Dalian University of Technology, Dalian, People's Republic of China

ABSTRACT

In this work, possible corrosion mechanisms of Fe- and Ni-based alloys are discussed which are protected by Cr_2O_3, NiO and MoO_2 surface layers. But chloride ions can dissolve these oxide films and there is a strong synergistic effect between hydronium ions and oxygen, leading to severe local alloy corrosion. On the other hand, titanium and Zr-3 alloys show good corrosion resistance in acidic oxidising subcritical water containing different inorganic salts. A double-layer oxide film (TiO and TiO_2) is formed on the surface of TA2 and TA9 alloys, while a triple oxide layer (TiO, Ti_2O_3 and TiO_2) is formed on TA10 surfaces in such aqueous solutions containing chloride and sulphate ions. In addition to the two oxide layers, $Ti_3(PO_4)_4$ deposits are also formed on the surface of TA2 and TA9 alloys when the subcritical water contains phosphates. Moreover, $(TiO)_2P_2O_7$ deposits form besides $Ti_3(PO_4)_4$ layers on the surface when the TA10 alloy is oxidised under the latter conditions.

ARTICLE HISTORY
Received 19 January 2018
Accepted 19 June 2018

KEYWORDS
Acidic oxidising subcritical water; corrosion; inorganic salt; titanium alloy; Zr-3 alloy

Introduction

A subcritical water oxidation process called Wet Air Oxidation (WAO) is considered to be a promising method for the removal of high concentrations of organic pollutants albeit acidic products are produced in the WAO reaction. It is generally carried out with or without catalyst at 120 – 320°C under pressures ranging from 0.5 to 20 MPa [1]. WAO is used for treatment of wastewaters containing toxic components and highly concentrated organics that are difficult to degrade by biochemical methods [2–4]. However, many chemical wastewaters contain inorganic anions (e.g. chloride ion, sulphate ion and phosphate ion) because of technical constraints. These inorganic salts can cause equipment corrosion which not only affects the safety of chemical operations but also causes economic losses to enterprises. It has been reported that corrosion problems will lead to huge losses in the global economy [5]. Up to now, many materials such as Ni-based alloys, stainless steel alloys, titanium alloys and zirconium alloys have been used for supercritical and subcritical water oxidation without salts [6–11]. However, little work has been done concerning the corrosion behaviour in subcritical water with high concentrations of inorganic salts. Thus, we have studied the effect of inorganic anions on the corrosion behaviour of equipment materials in subcritical water oxidation processes. This study will be beneficial to the selection of suitable equipment materials for industrial WAO applications.

Materials and methods

Materials and procedures

The details of the conditions used for corrosion tests are summarised in Table 1. The alloy specimen size was L × W × H = 15 × 5 × (3 – 4) mm^3. To simulate the WAO environment, an aqueous solution with 10% volume fraction hydrogen peroxide (30 wt-%, Tianda Chemical Co. Ltd) was used as an oxidant. Sodium chloride (≥99.5 wt-%, Kermel Chemical Co. Ltd), sodium sulphate (≥99.0 wt-%, Kermel) or sodium triphosphate (≥98.0 wt-%, Kermel) were added as the corrosive species. When organic phosphorus wastewater is degraded by WAO, most of the organic phosphorus is converted into inorganic phosphorus. Therefore, the investigation of the corrosion behaviour of the specimen under subcritical water with phosphate present is also relevant to WAO degradation of wastewater with organic phosphorus. The corrosion medium volume was 20 mL cm^{-2} of the specimen. In order to examine the corrosion resistance of the specimen under harsh conditions, the pH of the solution was adjusted to 0.4 using sulphuric acid (≈98.0 wt-%, Kermel) and the concentration of inorganic salt was close to the saturated solubility at room temperature. The experiments were carried out in a hydrothermal kettle with polytetrafluoroethylene lining (100 mL). After each corrosion test, the specimen was washed with deionised water and dried at 120°C for 2 h.

Analytic methods

Corrosion rates of all metals were evaluated using gravimetric methods as Equation (1).

$$v_L = \frac{\bar{v}}{\rho} \times \frac{24 \times 365}{1000} = 8.76 \times \frac{\bar{v}}{\rho} \quad (1)$$

v_L: Corrosion rates, mm/year; ρ: The density of the specimen, g cm^{-3}; $\bar{v}$: Weight loss index, g m^{-2} h^{-1}.

Scanning electron microscopy (SEM) images were obtained using a FE-SEM SUPRA 55 instrument from Carl Zeiss Jena. Energy-dispersive X-ray spectroscopy was carried out on an EDAX silicon-drift detector, which enabled rapid

CONTACT Chenglin Sun clsun@dicp.ac.cn
© 2018 Institute of Materials, Minerals and Mining Published by Taylor & Francis on behalf of the Institute

Table 1. Experimental conditions of corrosion tests.

Exp run no.	Alloy	Dissolved sodium chloride (wt-%)	Dissolved sodium sulphate (wt-%)	Dissolved sodium triphosphate (wt-%)	Temperature (°C)	Exposure time (h)
1	Zr-3	15	0	0	190	170
	2205	15	0	0	190	170
	Hastelloy C276	15	0	0	190	170
	Nickel-N6	15	0	0	190	170
	TA2	15	0	0	190	170
	TA9	15	0	0	190	170
	TA10	15	0	0	190	170
	316 SS	15	0	0	190	170
2	Zr-3	15	0	0	190	170
	TA2	15	0	0	190	170
	TA9	15	0	0	190	170
	TA10	15	0	0	190	170
3,4	Zr-3	0	15	0	190	170
	TA2	0	15	0	190	170
	TA9	0	15	0	190	170
	TA10	0	15	0	190	170
5,6	Zr-3	0	0	9	190	170
	TA2	0	0	9	190	170
	TA9	0	0	9	190	170
	TA10	0	0	9	190	170

determination of elemental compositions and acquisition of compositional maps of the specimens before and after corrosion.

X-ray photoelectron spectroscopy (XPS) was carried with a Thermo Scientific ESCA Lab250 instrument, which uses Al Kα radiation as the excitation source. XPS was performed to analyse the composition and chemical state of the surface elements of the specimens before and after corrosion. The binding energies were calibrated by setting the C1s band at 284.6 eV.

Results and discussion

All corrosion tests were conducted as subcritical water oxidation at 190°C. Based on the corrosion test results, a mechanism was developed for the effect of inorganic anions on the corrosion behaviour of equipment materials. The corrosion rates and surface chemical properties of the equipment materials and the mechanism describing their corrosion resistance are presented in this paper.

Corrosion rates

Sodium chloride is the most common salt in chemical wastewater. First, corrosion experiments were conducted on all the alloys using sodium chloride as corrosion medium. The corrosion rates for all tested alloys under the *Experiment 1* conditions are summarised in Table 2. With coexisting oxygen, hydronium and chloride ions, the corrosion resistance follows the order: Zr-3 > Titanium alloys > Hastelloy C-276 > 2205 > Nickel-N6 > 316 SS. This is in agreement with a previous study [12]. The guarantee period of industrial equipment years is 10 years, and the corrosion allowance of industrial devices is 0.5 mm at present. So, the acceptable corrosion depth of the materials is limited to less than 0.05 mm/year. Under the experimental conditions of *Experiment 1*, only the titanium and Zr-3 alloys meet this requirement. The Hastelloy alloy, 2205 duplex stainless steel, Nickel-N6 and stainless steel are not suitable for use in subcritical water oxidation environments with high sodium chloride contents. Therefore, in the following experiments, the corrosion resistance of the titanium and Zr-3 alloys was mainly investigated.

Table 2. Corrosion rates of all alloys under condition of *Experiment 1*.

Alloys	v^- (g m^{-2} h^{-1})	v_L (mm/year)
Zr-3	−0.0006	−0.0008
2205	3.4170	3.7416
Hastelloy C276	2.0284	1.9988
Nickel-N6	4.5041	4.4382
TA2	0.0046	0.0089
TA9	0.0098	0.0190
TA10	0.0081	0.0157
316 SS	4.4344	4.8678

Note: a negative value indicates weight gain of the tested specimen, and a positive value indicates weight loss.

It can be observed from Figure 1 that the second corrosion rates of all specimens are smaller than the first corrosion rates in a given corrosive medium indicating that some corrosion-resistant matter has been formed during the first corrosion test. All tested specimens exhibited weight loss in the corrosive 15 wt-% sodium sulphate solution but Zr-3, TA2 and TA9 still met the industrial requirements. In contrast, the tested specimens gained weight in the corrosive 9 wt-% sodium phosphate solution. The weight gain of the three kinds of titanium alloys was more than 0.05 mm/year, respectively, and only the weight gain of Zr-3 was less. The above results indicate that titanium and Zr alloys are suitable for the subcritical water containing sodium chloride. The Zr-3 and TA9 alloys are also suitable for the subcritical water containing sodium

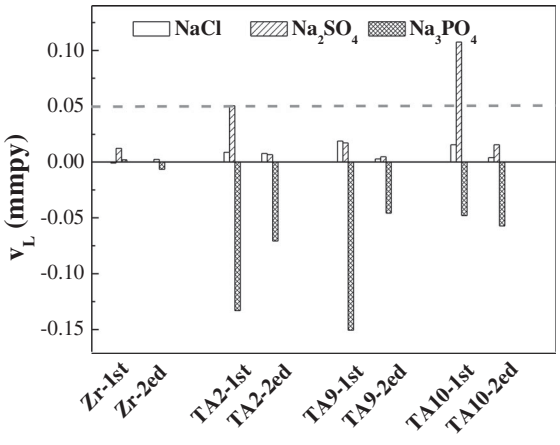

Figure 1. Corrosion rates of titanium and Zr-3 alloys in presence of different inorganic salts (*Experiments 1–6*).

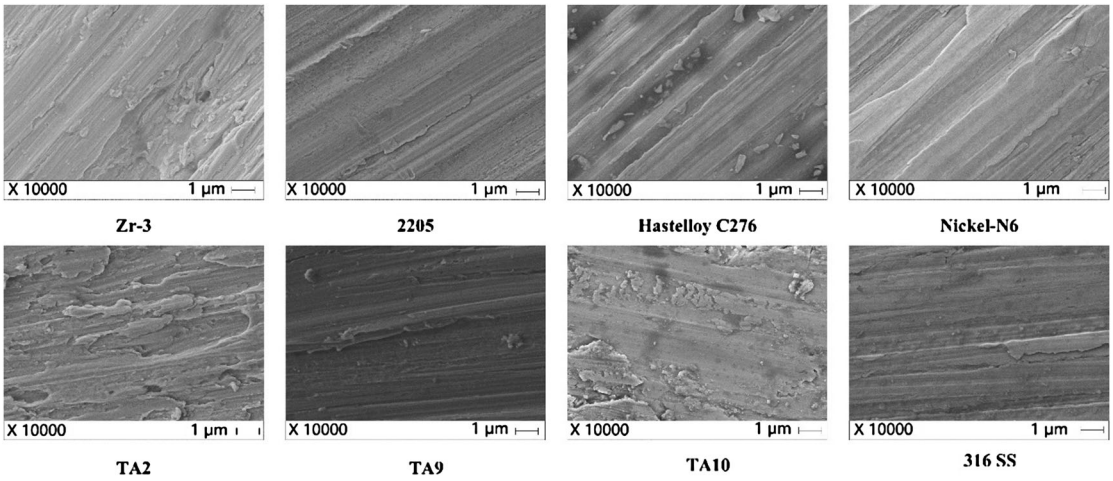

Figure 2. Surface morphologies of tested alloys before exposure to a corrosive medium.

sulphate, while the Zr-3 alloy is suitable for the subcritical water containing Na_3PO_4.

In order to understand the relationship between the mechanism of corrosion resistance and the surface properties of the alloys, detailed characterisation of the tested alloys was carried out. The results are discussed in the section below.

Surface properties of tested alloys

From the SEM images in Figure 2, it can be seen that all surfaces of the tested alloys were smooth at 10 000× magnification except for sanding patterns before exposure to the corrosive medium.

After *Experiment 1*, a blue oxide film appeared on the surface of the Zr3 and titanium alloys. The surface of duplex stainless steel 2205 and stainless steel 316L showed the greatest extent of corrosion because the metal came off. The surface of Nickel-N6 obviously suffered from pitting corrosion. Hastelloy C276 also exhibited the phenomenon of metal shedding and the metal colour became deeper.

From the SEM images in Figure 3, it can be seen that the morphology of these specimens changed greatly after *Experiment 1*. Spherical, flower-shaped and irregular granular matter had formed on the surface of the specimen which may be due to metal dissolution and oxidation. Pitting corrosion and crack corrosion occurred on the surface of the specimens, both of which are part of local corrosion. Pitting not only reduces the bearing capacity of the equipment but also may cause the explosion of pressure equipment. Oxidation reactions occurred in the cracks due to deposition of salt on solid metal surface. The oxidation reaction is accompanied by hydrogenation which results in the corrosive formation of long, at maximum 0.1 mm wide slits.

The surface compositions (in wt-%) of some alloys (316 SS, 2205, Hastelloy C276, Nickel-N6) are shown in Table 3 before and after *Experiment 1*. According to the results, most of the Cr and Mo transferred to the surface of the 2205 duplex stainless steel specimen which was seriously oxidised, while the content of Ni was reduced on the surface. The surface of the C-276 Hastelloy alloy specimen was seriously oxidised. Most of the Mo appeared on the surface of the specimen but the surface concentrations of Cr, Fe and especially Ni decreased. The C-276 Hastelloy alloy is not suitable for use in subcritical water oxidation with high sodium chloride amounts present

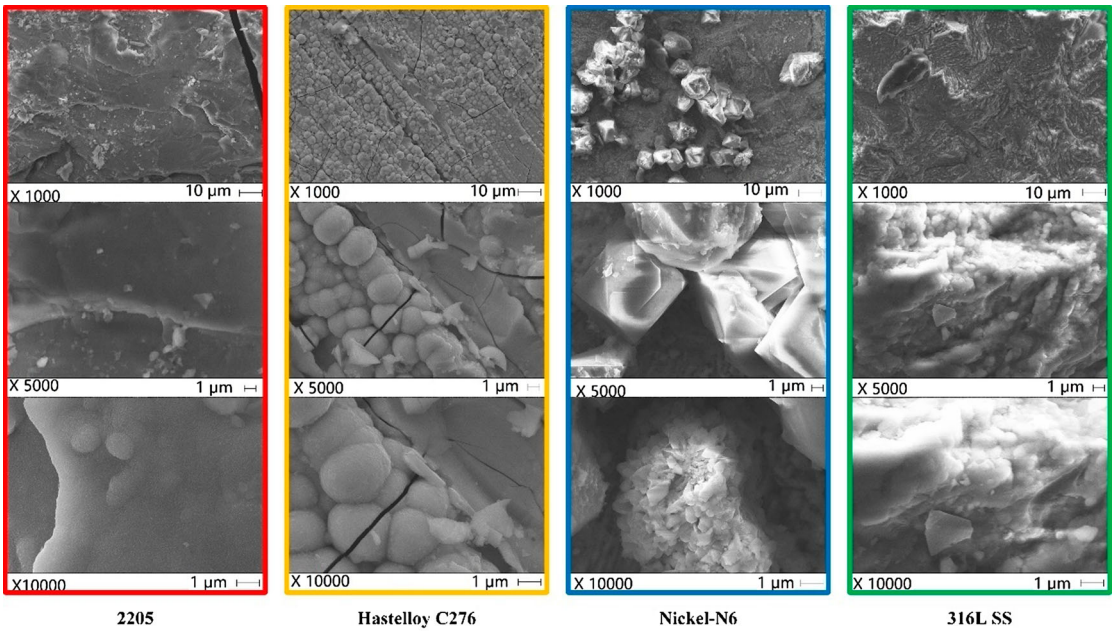

Figure 3. Surface morphologies of alloys (316 SS, 2205, Hastelloy C276, Nickel-N6) tested in *Experiment 1*.

Table 3. Surface compositions of 316 SS, 2205, Hastelloy C276 and Nickel-N6 alloys before and after *Experiment 1* (in wt-%).

	Element	Before	Element	After
2205	O	1.56	O	40.14
	Cr	23.52	Na	0.89
	Fe	66.08	Cl	1.20
	Ni	5.76	Cr	46.52
	Mo	3.09	Mo	11.24
Hastelloy C276	Cr	16.30	O	32.57
			Na	0.48
	Fe	5.84	Cl	0.69
			Cr	6.88
	Ni	57.28	Ni	1.73
	Mo	16.78	Mo	51.10
	W	3.80	W	6.54
Nickel-N6	O	0.70	O	20.74
			Na	5.07
	Ni	99.3	Cl	1.11
			Ni	73.08
316 SS	O	2.10	O	54.11
			Na	0.49
	Cr	18.83	Cl	1.20
	Fe	71.25	Cr	43.31
	Ni	7.83	Ni	0.89

because Mo oxides are unstable above 200°C [9]. The surface oxidation of Ni-N6 and 316L stainless steel was also serious after corrosion. Most of Cr in 316L stainless steel had transferred to the surface. In acidic solutions, the oxides and hydroxides of Cr(III) are thermodynamically stable above 250°C thus forming a protective film on the surface of Fe-based alloys.[13] The high corrosion rates of these alloys reflect the decreasing protective character of the Cr(III) oxide films in the presence of high sodium chloride concentrations. Pitting corrosion occurs when a critical pitting temperature is exceeded. For Fe-based alloys, the pitting corrosion temperature is 50°C and for Ni-based alloys, it is 100°C [14]. A study on the influence of chloride ion concentration on the electrochemical corrosion behaviour of titanium–zirconium–molybdenum alloy showed that Cl^- corrosion effectively destroys the passivating film formed on the TZM alloy surface [15].

In summary, Cr and Mo tend to form oxide films on the surface of Fe- or Ni-based alloys containing Cr and Mo in subcritical water with chloride ions present to protect the matrix elements, but these oxide films are unstable. When the specimen contains only Ni, the matrix is protected by forming a NiO oxide film on the surface. However, NiO is stable only in neutral and weakly alkaline environments and unstable in acidic environment [9].

The subsequent corrosion experiments focus on the corrosion resistance of Zr3, TA2, TA9 and TA10 alloys in subcritical water with high corrosive salt concentrations.

From the SEM images in Figure 4, it can be seen that the morphology of the Zr-3, TA2, TA9 and TA10 specimens changed slightly after *Experiment 2*. Small particles appeared on the surface of Zr-3, TA9 and TA10 while tetragonal particles appeared on the surface of TA2. The formation of small particles on the surface of the specimen may be caused by formed oxides.

The surface compositions (in wt-%) of the Zr-3, TA2, TA9 and TA10 alloys before and after *Experiment 2* are shown in Table 4. Both the titanium and Zr-3 alloys could prevent the matrix corrosion through formation of oxide films on the surface.

From the SEM images in Figure 5, it can be seen that the morphology of the Zr-3, TA2, TA9 and TA10 specimens changed slightly after *Experiment 4*. Small particles appeared on the surface of TA2, TA9 and TA10, while no particles appeared on the surface of Zr-3. The formation of small particles on the surface of the specimen may be caused by surface oxidation of the matrix.

Table 4. Surface compositions of titanium and Zr-3 alloys before and after *Experiment 2* (in wt-%).

	Element	Before	Element	After
	Zr	94.59	Zr	81.07
			O	18.83
	O	5.41	Na	0.01
Zr-3			Cl	0.09
	Ti	95.51	Ti	80.08
			O	19.48
	O	4.49	Na	0.07
TA2			Cl	0.05
	Ti	93.67	Ti	78.96
TA9	O	6.33	O	21.04
	Ti	89.56	Ti	75.73
TA10	O	10.44	O	24.27

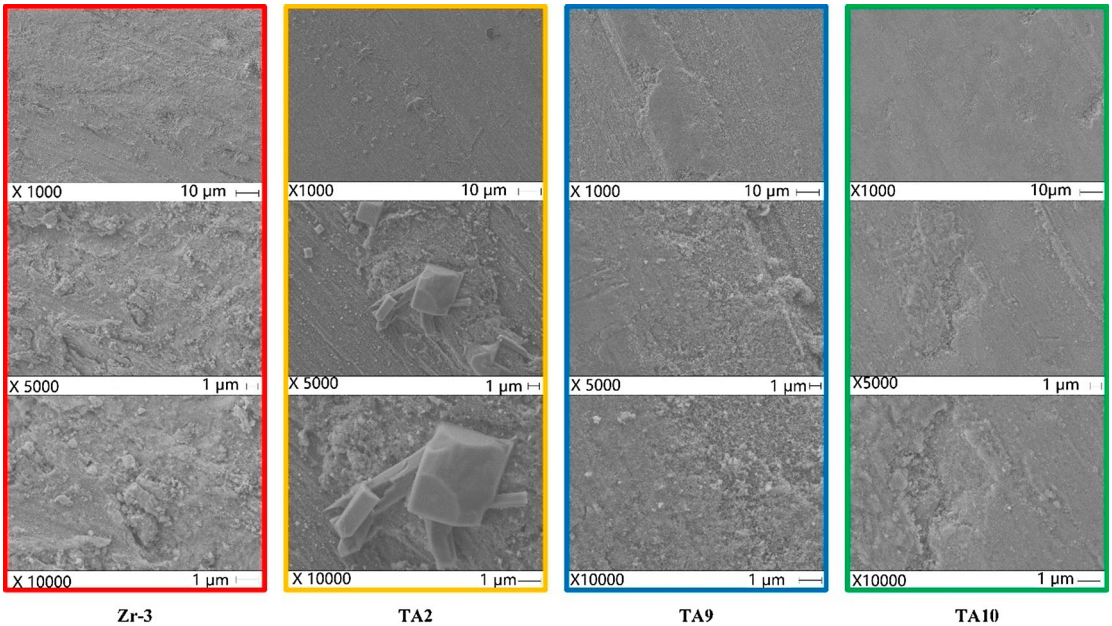

Figure 4. Surface morphologies of titanium and Zr-3 alloys after *Experiment 2*.

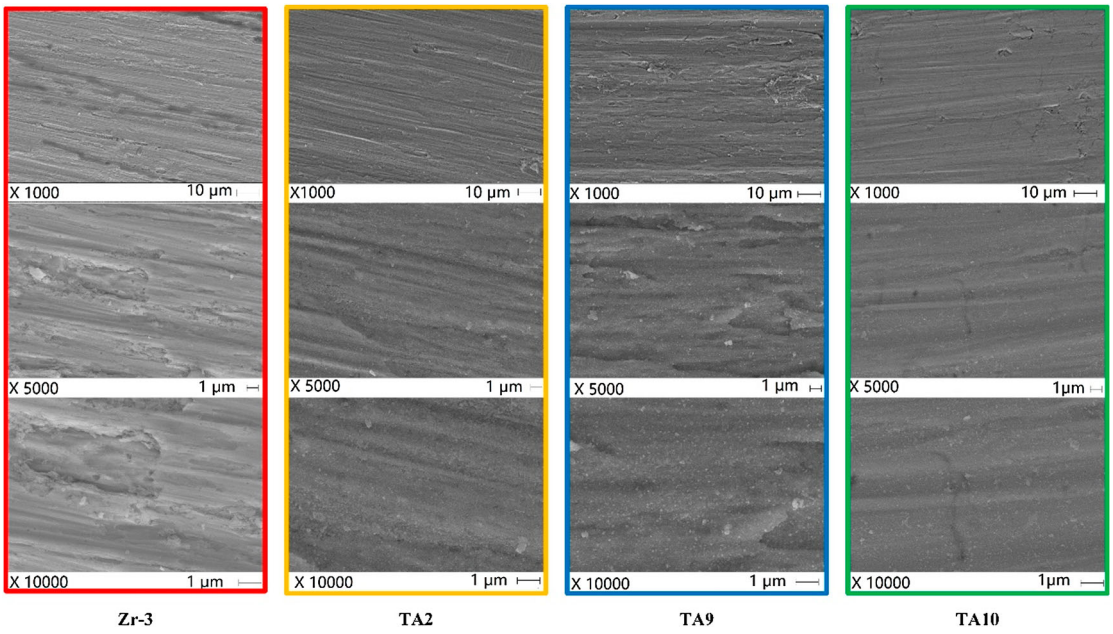

Figure 5. Surface morphologies of titanium and Zr-3 alloys after *Experiment 4*.

Table 5. Surface compositions of titanium and Zr-3 alloys before and after *Experiment 4* (in wt-%).

	Element	Before	Element	After
Zr-3	Zr	94.59	Zr	80.19
			O	17.60
	O	5.41	Na	1.16
			S	1.05
TA2	Ti	95.51	Ti	71.30
			O	28.58
	O	4.49	Na	0.03
			S	0.09
TA9	Ti	93.67	Ti	69.29
			O	30.62
	O	6.33	Na	0.02
			S	0.08
TA10	Ti	89.56	Ti	72.38
			O	27.33
	O	10.44	Na	0.07
			S	0.22

The surface compositions (in wt-%) of the Zr-3, TA2, TA9 and TA10 alloys before and after *Experiment 4* are shown in Table 5. Both the titanium and Zr-3 alloys could prevent the matrix from further corrosion through oxide formation on the surface. The content of oxygen on the surface of the titanium alloys is higher than that on Zr-3.

From the SEM images in Figure 6, it can be seen that the morphology of the Zr-3, TA2, TA9 and TA10 specimens changed greatly after *Experiment 6*. Tetragonal particles appeared on the surface of Zr-3, while tetragonal particles and 'pine needle-like' substances appeared on the surface of the titanium alloys.

The surface compositions (in wt-%) of the Zr-3, TA2, TA9 and TA10 alloys before and after *Experiment 6* are shown in Table 6. The formation of tetragonal particles on the surface of the specimen may be caused by surface oxidation of the matrix because the content of oxygen on the surface of the tested alloys was higher than that on the fresh specimen. A

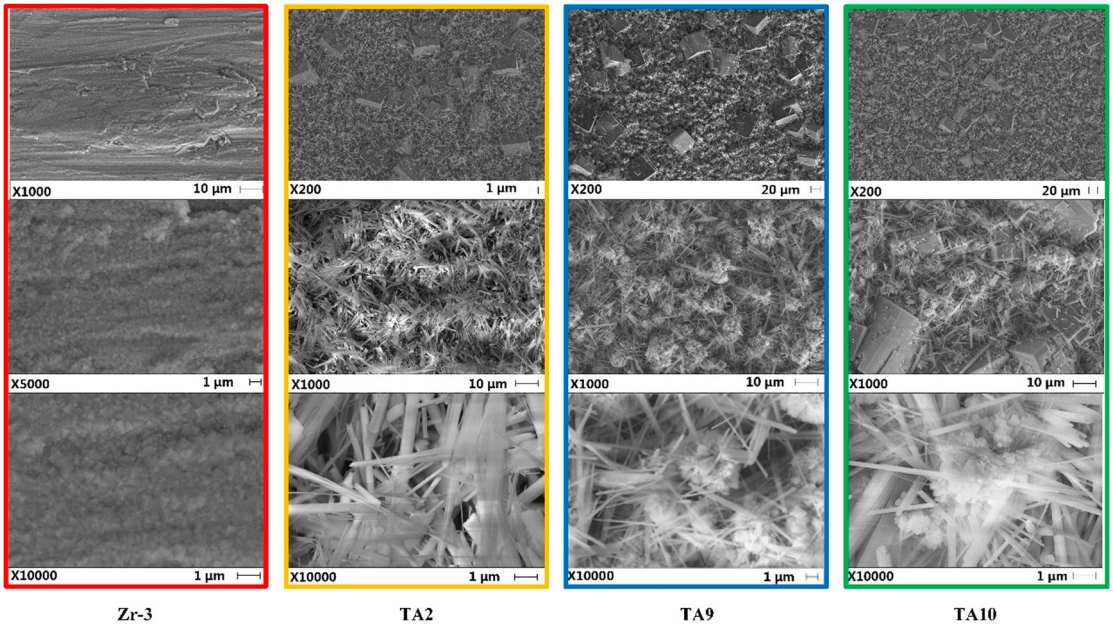

Figure 6. Surface morphologies of titanium and Zr-3 alloys after *Experiment 6*.

Table 6. Surface compositions of titanium and Zr-3 alloys before and after *Experiment 6* (in wt-%).

	Element	Before	Element	After
Zr-3	Zr	94.59	Zr	64.24
			O	28.46
	O	5.41	Na	1.58
			P	5.72
TA2	Ti	95.51	Ti	31.12
			O	49.82
	O	4.49	Na	0.34
			P	18.72
TA9	Ti	93.67	Ti	32.41
			O	49.57
	O	6.33	Na	0.10
			P	17.93
TA10	Ti	89.56	Ti	30.58
			O	50.83
	O	10.44	Na	0.24
			P	18.36

lot of phosphor appeared on the surface of the titanium alloys which indicates that phosphates deposited on the surface of the titanium alloys. Therefore, the 'pine needle-like' substances in Figure 6 may be phosphate deposits.

In conclusion, the corrosion resistance of Zr-3 is better than that of the titanium alloys in subcritical water which contains phosphates.

Surface chemical analysis of tested alloys

Ti has a strong resistance to local corrosion [16]. XPS analysis was performed to get a better understanding of the chemical state of Ti before and after the corrosion experiments. Figure 7 shows the XPS spectra of the fresh titanium alloys. The binding energy of about 459 eV could be attributed to Ti^0. The peaks at 462 and 457 eV could be assigned to Ti^{3+}, the one at 464 eV could be assigned to Ti^{4+} and the one at 454 eV could be assigned to Ti^{2+} [17]. The Ti^{2+} and Ti^{3+} species are associated with Ti suboxides and the Ti^{4+} species correspond to TiO_2. It can be clearly seen that metallic Ti is the main component before the corrosion experiments with only a small amount of TiO_x on the surface of the alloys.

In the subcritical water containing inorganic ions, Ti and TiO could be oxidised to TiO_2 or Ti_2O_3 on the surface of titanium alloys as indicated by Figures 8–10 (A)–(C1). Ti_2O_3 would be covered by lower layers of TiO_2. Therefore, the matrix would not be further corroded through the formation of a TiO_2 layer. In the phosphate-containing corrosion medium, PO_4^{3-} could deposit on the surface of TA2 and TA9 as shown by Figures 8 and 9 (C2). In addition to PO_4^{3-}, there is also $P_2O_7^{4-}$ on the surface of TA10. The above results are consistent with the results in the 'Surface properties of tested alloys' section .

Corrosion mechanism of tested alloys

There are three kinds of corrosion mechanisms known: the oxide film growth mechanism, the metal dissolution mechanism and the metal salt deposition mechanism [18–20]. In the present work, Zr-3, 2205, 316SS, Hastelloy C276, Nickel-N6 and titanium alloys were tested to investigate the corrosion mechanism in subcritical water containing inorganic anions.

To distinguish between a simultaneous and a synergistic action of two corrosive species, several groups of supplementary experiments were carried out with the TA2 alloy. WAO reactions are usually carried out in acidic oxidation conditions in subcritical water, and sodium chloride is the most common salt in chemical wastewater. Therefore, we consider hydrogen peroxide and hydronium ions as one combined corrosive agent and chlorine ion as another corrosive species in the actual WAO environment. The details of the supplementary corrosion tests are summarised in Tables 7 and 8.

In *Experiment 1*, the corrosion rate of TA2 is 0.0089 mm/year under the condition of A + B + C. We know from these

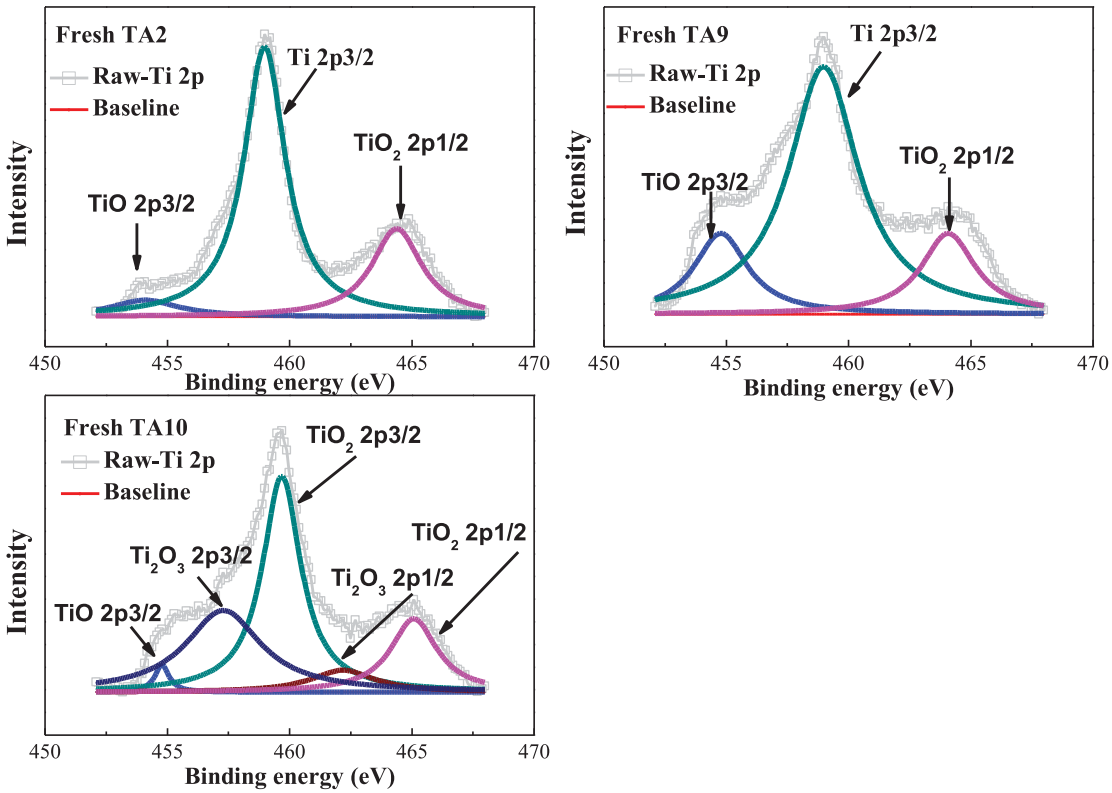

Figure 7. Surface chemical analysis of the fresh titanium alloys.

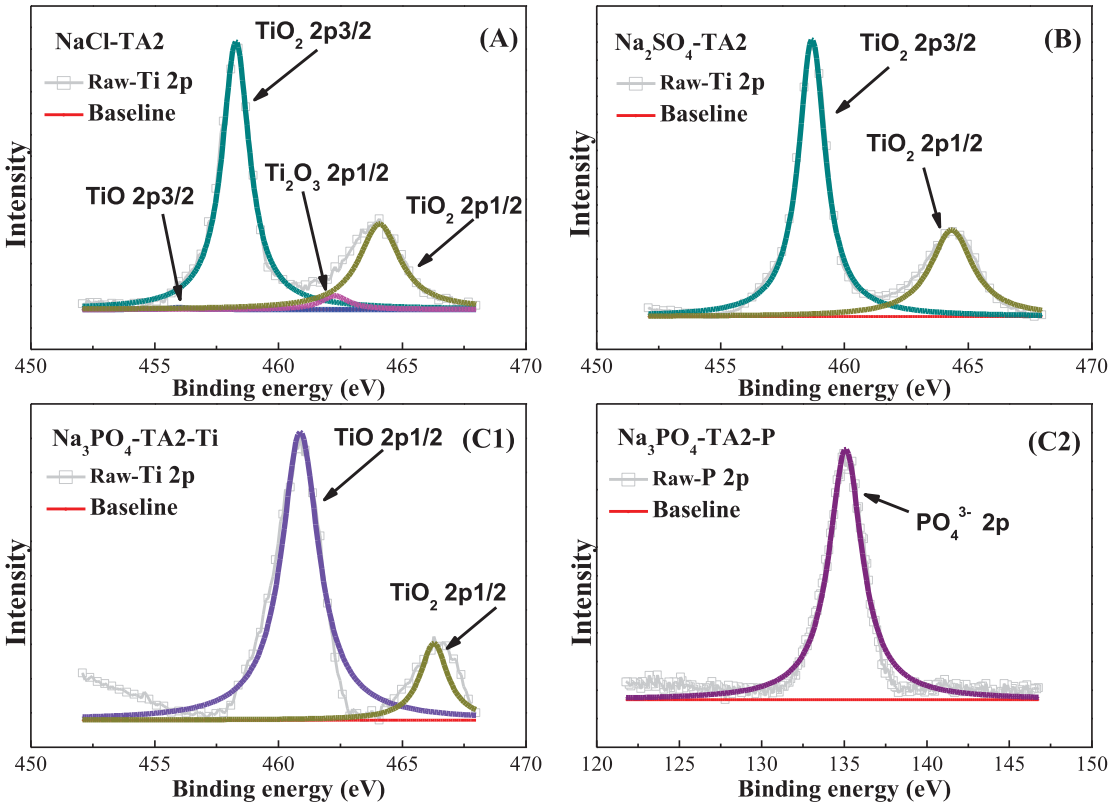

Figure 8. Surface chemical analysis of the TA2 alloy after *Experiments 2, 4 and 6*.

results that $v_L(A + B + C) < v_L(A) + v_L(B) + v_L(C)$ and $v_L(A + B) > v_L(A) + v_L(B)$. Therefore, hydrogen peroxide and the hydronium ion are together more corrosive than they are alone or the sum of their individual effects. So, there was a synergistic action of hydrogen peroxide and the hydronium ion. But there exists an antagonism between hydrogen peroxide, the hydronium ion and the chloride ion.

The morphology of the specimens before and after corrosion tests is compared in Figure 11 to distinguish between the precipitation of a corrosion product and the formation thereof. The surface of titanium alloys was shiny blue after *Experiment 2* and *Experiment 4*. This is due to the formation of metal oxides during the corrosion process. It can be seen that after *Experiment 6*, white corrosion products had precipitated on the

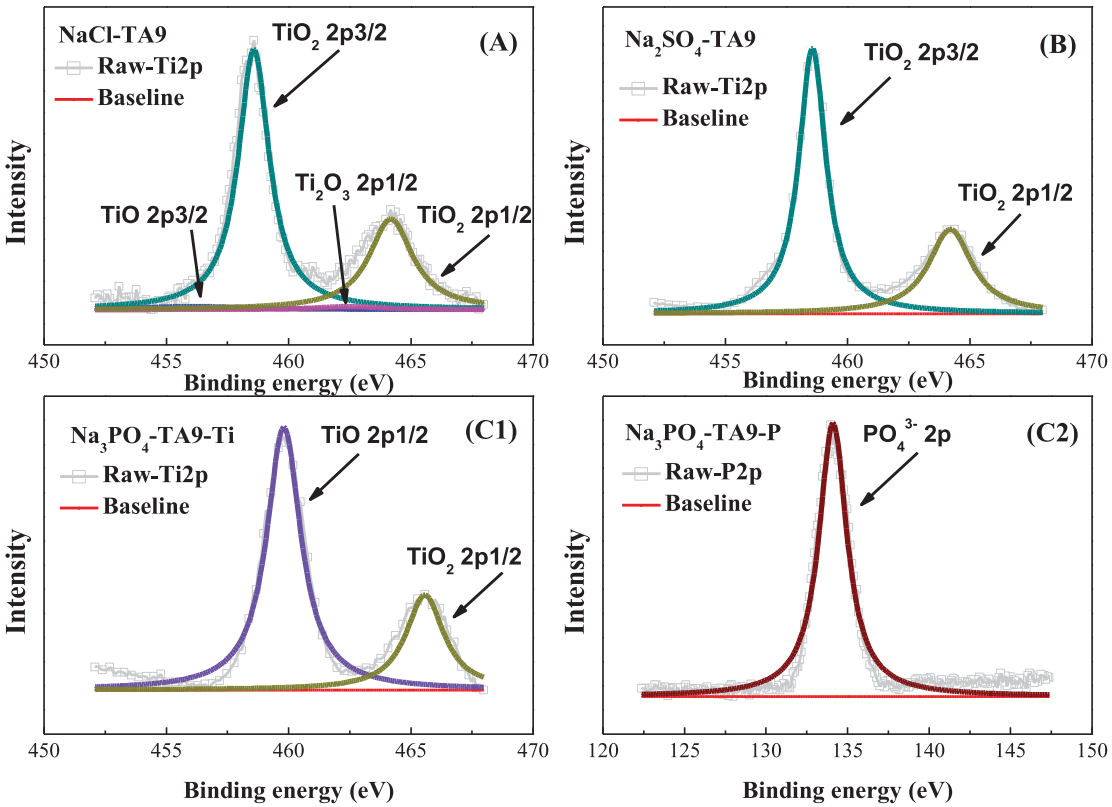

Figure 9. Surface chemical analysis of the TA9 alloy after *Experiments 2, 4 and 6*.

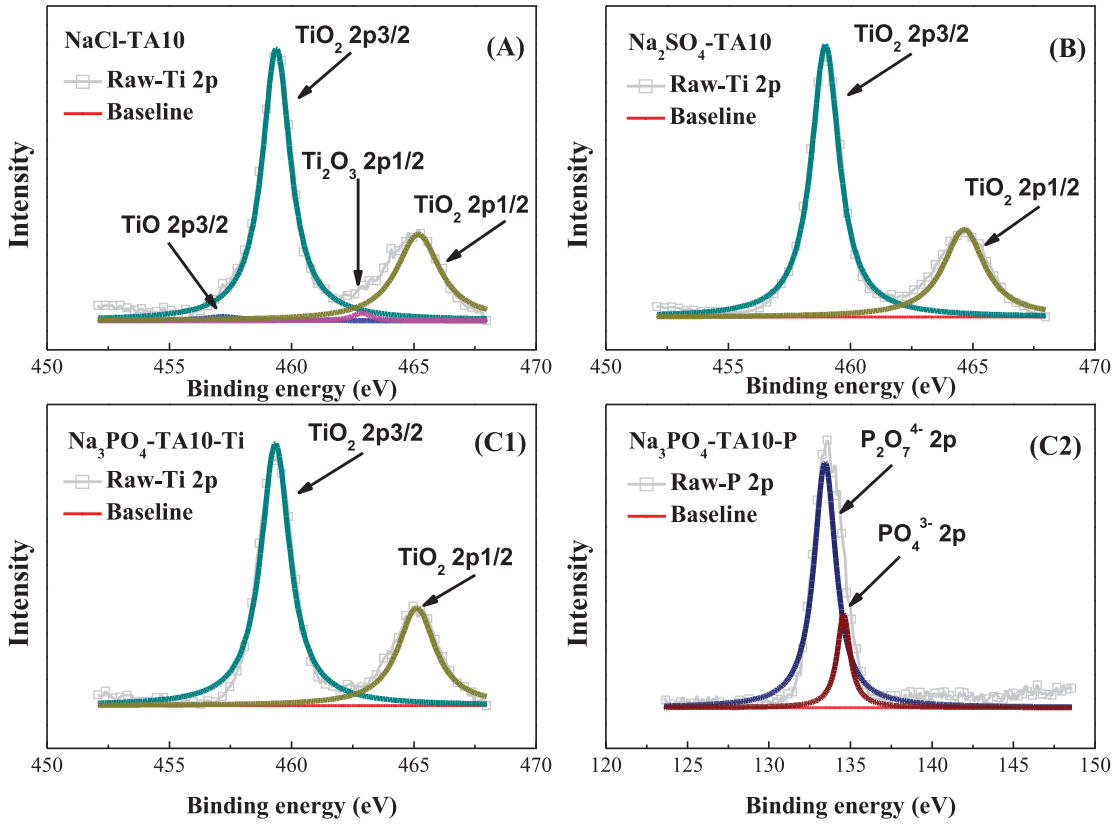

Figure 10. Surface chemical analysis of the TA10 alloy after *Experiments 2, 4 and 6*.

Table 7. Supplementary corrosion tests.

Exp run no.	7	8	9	10
Experimental conditions	A	B	A + B	C

A: 10% volume fraction hydrogen peroxide; B: Water solution of pH = 0.4; C: sodium chloride concentration = 150 g L^{-1}.

Table 8. Corrosion rates of supplementary corrosion tests.

Exp run no.	7	8	9	10
vL (mm/year)	0.0111	0.0088	0.0262	0.0862

surface of all tested alloys except Zr-3. This result is in agreement with the results of Figure 6 in the 'Surface properties of tested alloys' section which indicates the precipitation of phosphates. At the same time, a cubic phase appeared on the surface of the titanium alloys which may be due to the formation of titanium oxide. So, the corrosion test of *Experiment 6* suggests that there are two mechanisms for stabilisation of titanium alloys: the formation of titanium oxide and the precipitation of phosphates. On the other hand, the formation of metal oxides is the main mechanism in case of the Zr-3 alloy.

Figure 12 illustrates the possible corrosion mechanism of the tested alloys. 2205 and 316 SS are mainly composed of iron, chromium and molybdenum. The peeling of flakes could expose the alloy to the corrosive environment after *Experiment 1*. Although Cr_2O_3 and MoO_2 would be formed on the surface to protect the Fe-based alloys, the peeled area may be too large for the Cr_2O_3 to form an effective protection to the substrate. At the same time, Cr_2O_3 and MoO_2 are not stable in subcritical water with high concentrations of chloride ions, so that the further corrosion would occur. Hastelloy C276 and Nickel-N6 are nickel base alloys. The molybdenum in nickel base alloys enhances the resistance to pitting corrosion so that the matrix suffers less pitting

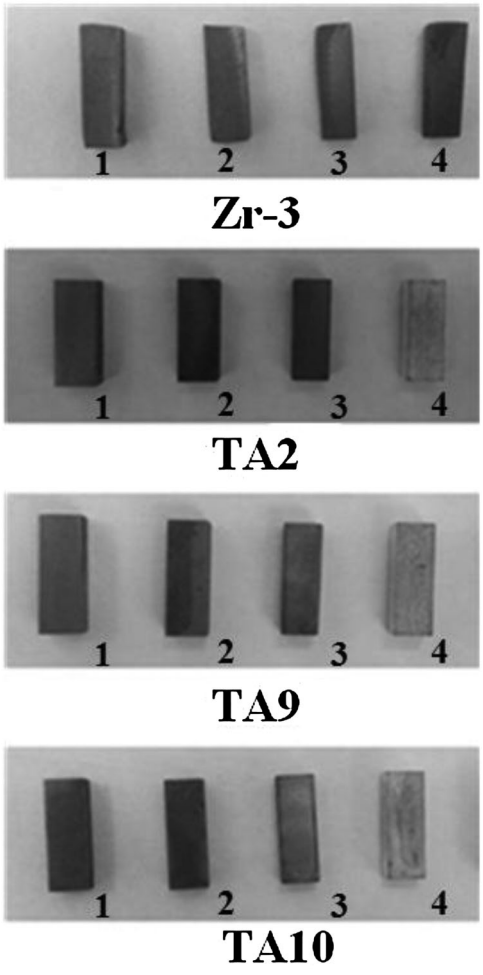

Figure 11. Comparison of specimens before and after corrosion tests (1: before corrosion experiments; 2: after Experiment 2; 3: after Experiment 4; 4: after Experiment 6).

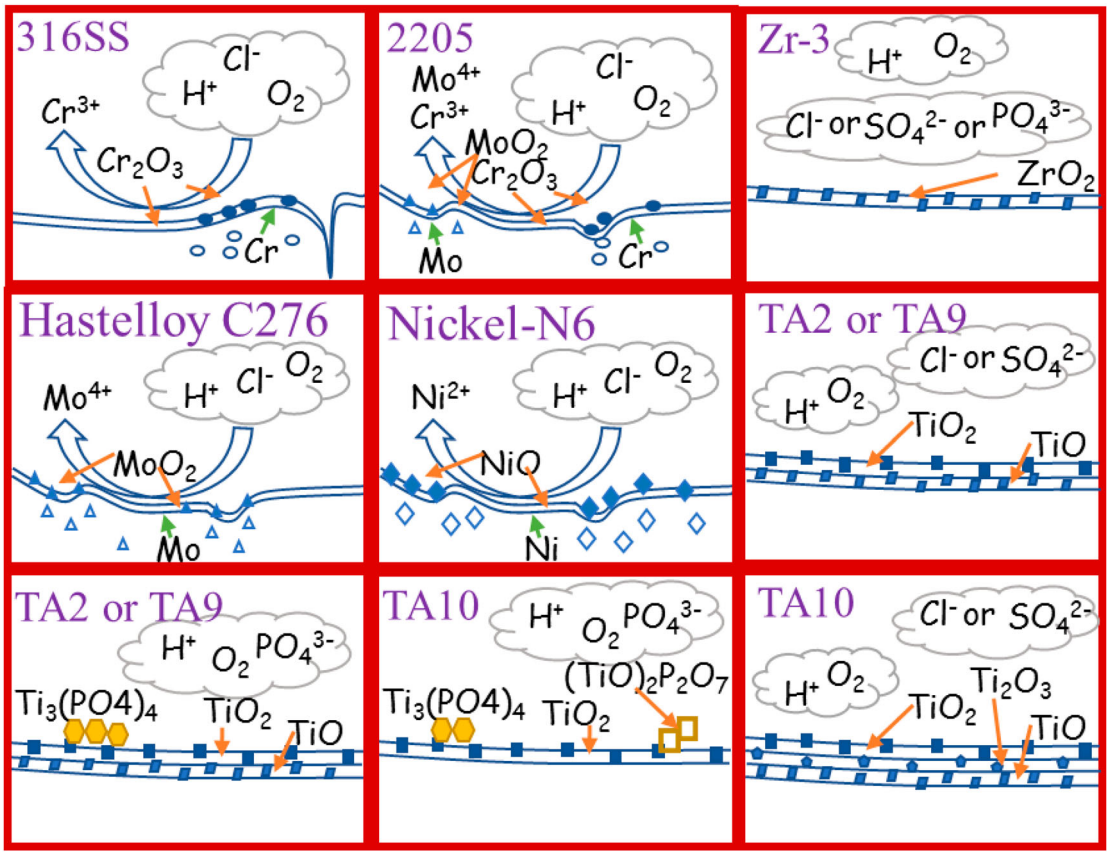

Figure 12. Corrosion mechanisms of tested alloys during exposure to subcritical water oxidation with high concentrations of chloride, sulphate and phosphate ions.

corrosion. The molybdenum could form the stable oxide MoO_2 to protect the substrate of Hastelloy C276. Ni is significantly depleted from the Nickel-N6 substrate and NiO could be formed on the surface of that specimen.

The zirconium alloy Zr3 shows the best corrosion resistance because a zirconium oxide film is uniformly formed on the surface. The mechanism of corrosion resistance is the same for the TA2 and TA9 alloys in the subcritical water oxidation environment containing different kinds of salts: a double-layer oxide film (consisting of TiO and TiO_2) is formed on the surface of them, and the oxygen content increased gradually from the inner to the outer oxide layer after *Experiment 2* and *Experiment 4*. In addition to the two layers of oxide film, $Ti_3(PO_4)_4$ deposits are also formed on the surface of the specimens after *Experiment 6*. In case of alloy TA10, a three-layer oxide film (TiO, Ti_2O_3 and TiO_2) is formed on the surface after *Experiment 2* and *Experiment 4*. The results show that the corrosion resistance has been largely improved, implying that titanium oxides play an important role in protecting the alloy matrix [21]. Moreover, in contrast with the behaviour of alloys TA2 and TA9, $Ti_3(PO_4)_4$ deposits form on the surface besides the oxide film and $(TiO)_2P_2O_7$ also appears as shown by Figure 10(C2) when the TA10 alloy is oxidised in subcritical water containing phosphate ions. This result is consistent with the reported corrosion mechanism of TA10 in subcritical water in that the titanium corrosion products consist of $Ti_5O_4(PO_4)$, $Na(Ti)_2(PO_4)_3$ and TiO_2.[22]

Conclusions

In this work, corrosion tests were performed with alloys Zr-3, TA2, TA9, TA10, Hastelloy C-276, 2205, Nickel-N6 and 316 SS under subcritical water containing high concentrations of inorganic salt. Changes in morphology and surface composition due to the corrosion experiments were explored. In subcritical water containing high chloride ion concentrations, Cr_2O_3 and MoO_2 layers will be formed on the surface to protect the Fe-based alloy substrate while Ni-based alloys are protected by NiO and MoO_2 layers. However, chloride ions cause local corrosion and dissolution of the MoO_2 and NiO layers on Ni-based alloys. Severe pitting corrosion is observed on the 2205 and 316SS alloys in subcritical saline aqueous solutions. In contrast, titanium and Zr-3 alloys show good corrosion resistance in subcritical water containing different salts due to the formation of stable surface oxide layers. At certain salt concentrations, the corrosion rate decreases when the specimen is exposed again to the same corrosion solution. Finally, the Zr-3 alloy is proposed as best engineering material for wastewater treatment by subcritical water that contains high concentrations of phosphates. Titanium alloys and the Zr-3 alloy are suitable for use in the subcritical water containing chloride ions, while the Zr-3 and TA9 alloys are suitable for use in the subcritical water containing sulphate ions.

Acknowledgement

The authors thank Professor Andreas Goldbatch for his help in editing.

Disclosure statement

No potential conflict of interest was reported by the authors.

Funding

This work was supported by the Major Science and Technology Projects of Shandong Province [grant number 2015ZDXX0402B01] and the Key Programs of the Chinese Academy of Sciences [grant number ZDRW-ZS-2016-5].

References

[1] Yang S, Besson M, Descorme C. Catalytic wet air oxidation of succinic acid over Ru and Pt catalysts supported on CexZr1-xO2 mixed oxides. Appl Catal B Environ. 2015 Apr;165:1–9.

[2] Fontanier V, Zalouk S, Barbati S. Conversion of the refractory ammonia and acetic acid in catalytic wet air oxidation of animal byproducts. J Environ Sci. 2011;23(3):520–528.

[3] Keav S, de los Monteros AE, BarbierJrJ, et al. Wet air oxidation of phenol over Pt and Ru catalysts supported on cerium-based oxides: resistance to fouling and kinetic modelling. Appl Catal B Environ. 2014 May 5;150:402–410.

[4] Wang S, Yang Q, Bai Z, et al. Catalytic wet air oxidation of wastewater of the herbicide fomesafen production with CeO2-TiO2 catalysts. Environ Eng Sci. 2015 May 1;32(5):389–396.

[5] Hou B, Li X, Ma X, et al. The cost of corrosion in China. npj Mater Degrad. 2017;1(1). doi:10.1038/s41529-017-0005-2.

[6] Jiang S, Huang X, Li W, et al. Effect of steam pressure on the oxidation behaviour of alloy 625. In: Liu X, Liu Z, Brinkman K, et al., editors. Energy Materials 2017. Minerals Metals & Materials Series. Cham: Springer; 2017. p. 329–341.

[7] Wang M, Wang SZ, Li YH, et al. Corrosion research on different types of nickel-base alloy and stainless steel in a wastewater under the condition of anaerobic subcritical. Energ Mech Eng. 2016;2016: 57–62.

[8] Li W, Huang X, Li J, et al. Effect of pressures on the corrosion behaviours of materials at 625A degrees C. JOM. 2017 Feb;69(2):207–216.

[9] Kritzer P, Boukis N, Dinjus E. The corrosion of nickel-base alloy 625 in sub- and supercritical aqueous solutions of oxygen: a long time study. J Mater Sci Lett. 1999 Nov;18(22):1845–1847.

[10] Kaul C, Vogel H, Exner HE. Corrosion behaviour of inorganic materials in subcritical and supercritical aqueous solutions. Materialwiss Werkst. 1999 Jun;30(6):326–331.

[11] Kritzer P, Schacht M, Dinjus E. The corrosion behaviour of nickel-base alloy 625 (NiCr22Mo9Nb; 2.4856) and ceria stabilized tetragonal zirconia polycrystal (Ce-TZP) against oxidizing aqueous solutions of hydrofluoric acid (HF), hydrobromic acid (HBr), and hydriodic acid (HI) at sub- and supercritical temperatures. Materi Corros. 1999 Sep;50(9):505–516.

[12] Tang X, Wang S, Qian L, et al. Corrosion behavior of nickel base alloys, stainless steel and titanium alloy in supercritical water containing chloride, phosphate and oxygen. Chem Eng Res Des. 2015;100:530–541.

[13] Kritzer NB P, Dinjus E. Review of the corrosion of nickel-based alloys and stainless steels in strongly oxidizing pressurized high-temperature solutions at subcritical and supercritical temperatures. Corrosion. 2000;56(11):1093–1104.

[14] Laycock MHM NJ, Newman RC. Metastable pitting and the critical pitting temperature. J Electrochem Soc. 1998;145(8):2622–2628.

[15] Hu P, Song R, Li X-J, et al. Influence of concentrations of chloride ions on electrochemical corrosion behavior of titanium-zirconium-molybdenum alloy. J Alloy Comp. 2017;708:367–372.

[16] Zhou S. Corrosion resistance investigation of titanium alloy as tissue engineered bone implant. Int J Electrochem Sci. 2017: 7174–7182. doi:10.20964/2017.08.61.

[17] Fu T, Wang X, Liu J, et al. Characteristics and corrosion behavior of pure titanium subjected to surface mechanical attrition. JOM. 2017;69(10):1844–1847.

[18] Yoon JH, Kim HS, Kim YS, et al. Influence of chromizing treatment on corrosion behavior of aisi 316 stainless steel in a supercritical water oxidation. Met Mater Int. 2004 2004;10(1):83–88.

[19] Tang X, Wang S, Xu D, et al. Corrosion behavior of Ni-based alloys in supercritical water containing high concentrations of salt and oxygen. Ind Eng Chem Res. 2013 Dec 25;52(51):18241–18250.

[20] Karmiol Z, Chidambaram D. Comparison of performance and oxidation of nitronic-50 and stainless steel 316 in subcritical and supercritical water environments. Metall Mater Transactions A Phys Metall Mater Sci. 2016 May;47A(5):2498–2508.

[21] Lu J. Enhanced corrosion resistance of TA2 titanium via anodic oxidation in mixed acid system. Int J Electrochem Sci. 2017: 2763–2776. doi:10.20964/2017.04.69.

[22] Jian-shu MZy Lu, Jiu-yuan Zhang, Chun-an MX-b Ma, et al. Corrosion of titanium in supercritical water oxidation environments. Transactions Nonferr Metal Soc China. 2002;06:1054–1057.